Magnetic Nanotubes

DOI: 10.1002/ange.200701671

Pt-Catalyzed Formation of Ni Nanoshells on Carbon Nanotubes**

Marek Grzelczak, Miguel A. Correa-Duarte, Verónica Salgueiriño-Maceira, Benito Rodríguez-González, José Rivas, and Luis M. Liz-Marzán*

Apart from their intrinsically interesting one-dimensional (1D) morphology, sp^2-bonded carbon nanotubes (CNTs) have remarkable, structure-dependent electronic, mechanical, optical, and magnetic properties[1] that make them promising components in nanocomposite architectures. CNTs have also found numerous other, already demonstrated applications in many different fields, including catalysis, sensors, semiconductor devices, biological environments, data storage/processing devices, and reinforced nanofiber materials.[2] CNT-based nanocomposites have been created by the assembly of a variety of nanoparticles (NPs) onto surface-primed CNTs. In most of these examples, the assembled NPs display mutual interactions but their individual nanosized nature is maintained within the resulting 1D CNT-based nanocomposites.[3,4] Among such nanocomposites, the combination of CNTs with magnetic materials offers an increased interest owing to the monodimensionality of the final composites, which results in an increase of the magnetic anisotropy, and the possibility of alignment under manipulation with external magnetic fields. Such aligned CNTs are particularly attractive for the design of, for example, new reinforced nanofiber materials.

CNTs can thus be used as unique templates for the synthesis of 1D magnetic nanomaterials, which have recently received considerable attention.[5] In particular, colloidal dispersions of anisotropic magnetic nanoparticles have been prepared by different techniques, such as: a) the selective control of the growth rates of different faces through relatively simple variations in surfactant composition;[5] b) the assembly of pre-formed magnetic nanoparticles into chains or necklaces through magnetic dipole–dipole interparticle interactions;[6] or c) the assembly of magnetic nanoparticles onto surface-modified CNTs through electrostatic interactions, which leads to the synthesis of anisotropic CNT-based magnetic composites.[3]

Whereas the use of pre-formed magnetic nanoparticles allows the selection of nanoparticles with well characterized magnetic properties, which can be maintained within the composite, these systems suffer from the inherently weak magnetic interaction between the small magnetic core volume of the nanoparticles involved. The decay of this dipole–dipole interaction potential between single magnetic particles is such that polyelectrolyte layers or even a silica shell only a few nanometers thick can minimize these interactions.[6g] An alternative method involves the growth of a continuous shell of a pre-selected magnetic material on a suitable anisotropic template, such as nanowires or nanotubes, so that the magnetic response is better defined all along the nanostructure.

Herein we present the synthesis of well-defined, anisotropic magnetic nanotubes, using CNTs as templates, in which the sp^2 carbon structure is preserved while obtaining a ferromagnetic behavior at room temperature. The magnetic material is grown directly on the CNT outer surface in a process that is mediated by an assembled layer of pre-synthesized, catalytic Pt nanoparticles. This intermediate step yields organic–inorganic hybrid composites which serve as 1D substrates for the preparation of magnetic CNT-supported Ni/

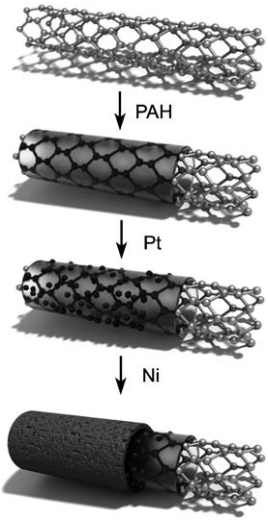

Figure 1. Illustration of the synthetic process comprising the polymer (PAH) wrapping of CNTs, electrostatic self-assembly of pre-synthesized Pt nanoparticles, and Ni reduction to form CNT-supported Ni/NiO nanoshells.

[*] M. Grzelczak, Dr. M. A. Correa-Duarte, Dr. B. Rodríguez-González, Prof. L. M. Liz-Marzán
Departamento de Química Física
Universidade de Vigo, 36310 Vigo (Spain)
Fax: (+34) 986-812-556
E-mail: macorrea@uvigo.es
Dr. V. Salgueiriño-Maceira, Prof. J. Rivas
Departamento de Química-Física y Física Aplicada
Universidade de Santiago de Compostela
15782 Santiago de Compostela (Spain)

[**] M.A.C.-D. and V.S.-M. are grateful to the Isidro Parga Pondal Program (Xunta de Galicia, Spain) for fellowships. This work was supported by the Spanish Xunta de Galicia (grant no. PGIDIT06PXIB314379PR), the Spanish Ministerio de Educación y Ciencia (Consolider Ingenio 2010, "Nanobiomed"), and by the European Commission Marie Curie RTN "SyntOrbMag" (contract no. MRTNCT-2004-005567). We thank Dr. C. Senra (CACTI, U. Vigo) for performing XPS measurements.

Supporting information for this article is available on the WWW under http://www.angewandte.org or from the author.

NiO nanotubes (Figure 1). Potential applications for Ni/Pt nanostructures include their use as catalysts,[7] in oxygen-reduction reactions within polymer electrolyte membrane fuel cells,[8] or in direct oxidation methanol fuel cells.[9] Moreover, CNT-supported Ni/NiO nanotubes could be used as electrodes that display high electrocatalytic activity for hydrogen peroxide detection in biosensing applications.[10] Suspensions of Ni nanowires have also been proposed as magneto-optical switches because of their ability to scatter light that is perpendicularly incident to the wire axis.[11] These nanowires, when ferromagnetic, have large remnant magnetization owing to their large aspect ratios and hence can be used in low-field environments where superparamagnetic beads do not perform at all.[12] Additionally, since these composite structures involve a Ni/NiO antiferromagnetic/ferromagnetic interface, an exchange bias effect is expected which could find promising applications in magnetoresistive devices.[13]

Figure 1 summarizes the experimental procedure, which involves three main steps. First, CNTs are functionalized by wrapping them with a positively charged polyelectrolyte (polyallylamine hydrochloride (PAH)), which then acts as a molecular glue for the attachment of negatively charged Pt nanoparticles onto the surface of the CNTs. These nanoparticles, in turn, serve as catalytic centers for Ni reduction. The so-called polymer wrapping technique is a noncovalent functionalization which, in contrast to defect-side- and covalent-side-wall functionalization, prevents the disruption of the nanotubes' intrinsic sp^2 conjugation, thereby preserving their electronic structure.[14] This polymer wrapping technique relies on the thermodynamic preference of CNT–polymer interactions over CNT–water interactions, whereas the second stage (attachment of the Pt nanoparticles) is based on an electrostatic and van der Waals attraction between the negatively charged nanoparticles and the positively charged PAH-functionalized surface of the CNTs.[15]

This strategy permits the assembly of pre-synthesized nanoparticles of varying morphology (size and shape), as required by each specific final application. Platinum-covered CNTs (CNT/Pt) with different Pt loadings can be obtained by controlling both the deposition time and the CNT:Pt nanoparticles concentration ratio during the deposition process. CNT/Pt nanocomposites were prepared from Pt nanoparticles with different sizes (see representative TEM images in Figure 2 and the Experimental Section), with homogeneous coatings of Pt nanoparticles over the complete surface of the CNTs invariably being obtained. While some small nanoparticle groups are observed (see Figure 2a), the Pt nanoparticles are, in general, uniformly distributed on the nanotubes with the same size distribution as in the original dispersion (see inset in Figure 2a). The size of the Pt nanoparticles (av. diameter: 5 nm) selected to demonstrate the homogeneous Ni reduction and CNT coating was chosen so that they could be identified during the subsequent coating steps, but smaller particles can also be used.

The CNT/Pt nanocomposites were used as templates for the preparation of Ni nanotubes by taking advantage of the catalytic behavior of small Pt seeds. Pt nanoparticles play a crucial role in the formation of metallic Ni on the walls of the

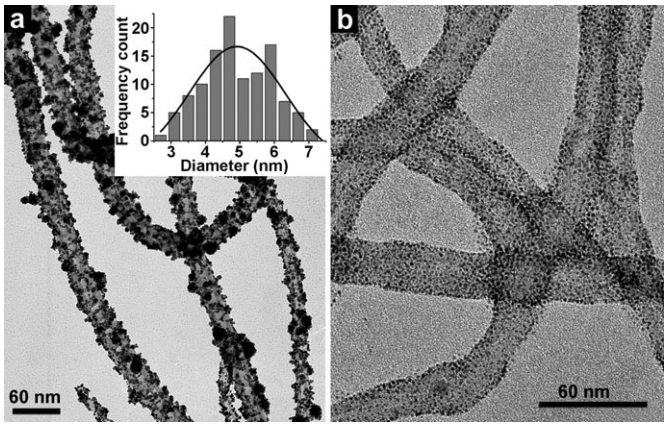

Figure 2. TEM images of CNT@Pt nanocomposites prepared by depositing 5- (a) and 2.5-nm (b) Pt nanoparticles. Inset in (a): size distribution of the 5-nm Pt nanoparticle dispersion.

CNTs by catalyzing the reduction of the Ni/hydrazine complex formed in aqueous solution, as described below. This reaction allows the CNT/Pt nanocomposites to be coated with a uniform and homogeneous Ni layer (ca. 10 nm thick), with no need for surfactants or other stabilizers in aqueous solution. This feature is relevant since the use of surfactants or other stabilizers usually hinders subsequent manipulation and implementation in different applications. The CNT/Pt@Ni composites reported herein are stable in solution (most likely because of the presence of a negatively charged NiO surface layer) and their surface is free of surfactants, thus allowing further functionalization where required.

Figure 3 shows representative TEM and HRTEM images of the CNT/Pt@Ni samples obtained following the process described above. These images clearly show the homogeneous

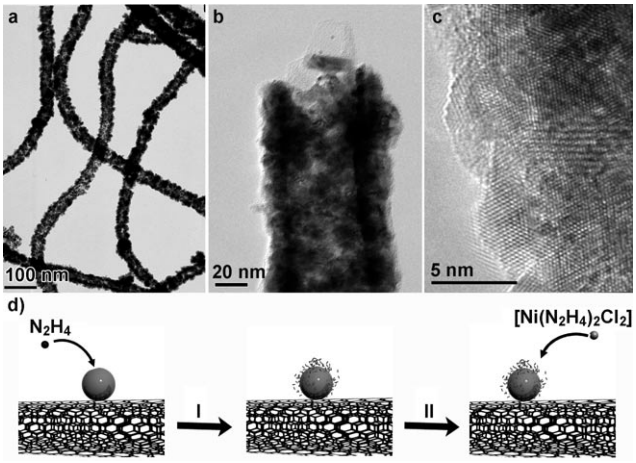

Figure 3. Representative TEM images a) of the CNT/Pt structures coated with a uniform outer layer of nickel (ca. 10 nm) and b) a detail of a CNT@Ni tip (b). c) HRTEM image showing the polycrystalline nature of the nickel shell deposited on the CNT/Pt nanocomposites. d) Illustration of Ni reduction on the CNT/Pt side-walls. Step I involves the decomposition of hydrazine on the surface of Pt nanoparticles, which results in a charged surface, and step II the reduction of the hydrazine/Ni complex on the charged Pt surface.

coating of individual CNTs and reveal the crystalline nature of the Ni layer in the final composite. Crystalline planes can be observed both in the darker areas (corresponding to the internal Pt nanoparticles) and over the whole surface of the nanocomposites, thereby reflecting the polycrystalline nature of the magnetic nanowires synthesized.

The proposed mechanism for the formation of metallic Ni on the surface of the Pt nanoparticles is depicted schematically in Figure 3d. Complexes between transition-metal ions and hydrazine are easily formed in water[16] and that such complexes can be decomposed in the presence of hydroxy groups,[17] in a process where Ni^{II} complexes are reduced to Ni^0. However, the catalytic decomposition of hydrazine in the presence of platinum nanoparticles can take place on the surface of these nanoparticles by an electrophilic addition, that is, by forming electrophilic radicals which can then react with other hydrazine molecules from solution.[18] The presence of metallic platinum nanoparticles therefore implies the reduction of nickel complexes without the need for additional hydroxy groups present in solution. In fact, we observed that reduction of Ni^{2+} did not occur in experiments using PAH-functionalized CNTs in the absence of Pt nanoparticles. Thus, the mechanism of Ni nanotube formation can be explained in the following terms: the excess hydrazine that is not complexed with Ni^{2+} ions can be catalytically decomposed on the surface of the platinum nanoparticles supported on the CNTs. This step generates a charged metallic surface (step I, Figure 3d) which promotes the reduction of the Ni^{II} complex into Ni^0 (step II, Figure 3d). Subsequent decomposition of hydrazine on the surface of the reduced metal is facilitated,[19] thus favoring further Ni reduction and growth of a homogeneous shell. The process terminates when all the Ni^{II} has been reduced. The advantage of this surface-catalyzed reduction of Ni^{II} is the formation of a continuous (though polycrystalline) Ni layer rather than an outer shell composed of nanoparticles, with an expected improvement of the resulting magnetic properties.

A scanning transmission electron microscopy (STEM) analysis of the samples was performed to confirm the formation of the expected core(CNT)/shell(Pt)@shell(Ni) structure. The dark-field STEM image (Figure 4a) shows a mass-thickness contrast, with brighter areas in the material close to the surface of the CNTs corresponding to Pt nanoparticles. STEM-XEDS (X-ray energy dispersion spectroscopy) elemental mapping of the hybrid structures (Figure 4b) shows the relative distribution of the elements, with red areas corresponding to Pt (Pt M_α line) and green areas corresponding to Ni (Ni K_α line). The image clearly shows that Pt is located on the inner side of the metallic shell with Ni mostly covering the outer part, as expected for the proposed onionlike structure.

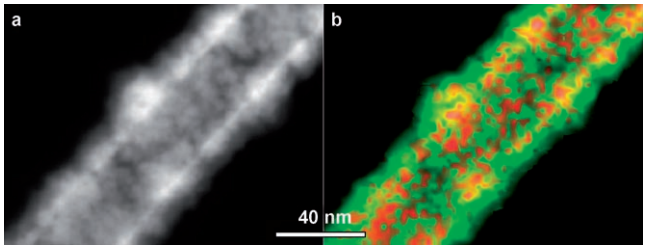

Figure 4. STEM analysis of the CNT/Pt@Ni nanostructures. a) Dark-field image where the Pt particles appear brighter. b) Elemental mapping by XEDS analysis, with Pt (M_α line) in red and Ni (K_α line) in green.

The analysis was completed with HRTEM images (Figure 5), where the multi-wall structure of the CNTs used in this procedure can clearly be seen. This procedure allowed us to determine a value for the interwall distance in the multi-walled nanotubes (MWNTs) of about 0.34 nm. This value agrees well with the interwall spacing of MWNTs reported by Kiang and co-workers,[20] which range from 0.34 to 0.39 nm depending on the diameter of the outer nanotubes, as well as with the interplanar distance of graphite (0.336 nm).[21] Interwall and interplanar distances were determined by Fourier transform analysis of the HRTEM image shown in Figure 5b for MWNTs (0.34 nm), Pt (0.22 nm), and Ni (0.20 and 0.17 nm), thereby confirming the pre-designed structure of the obtained CNT/Pt@Ni nanocomposites.

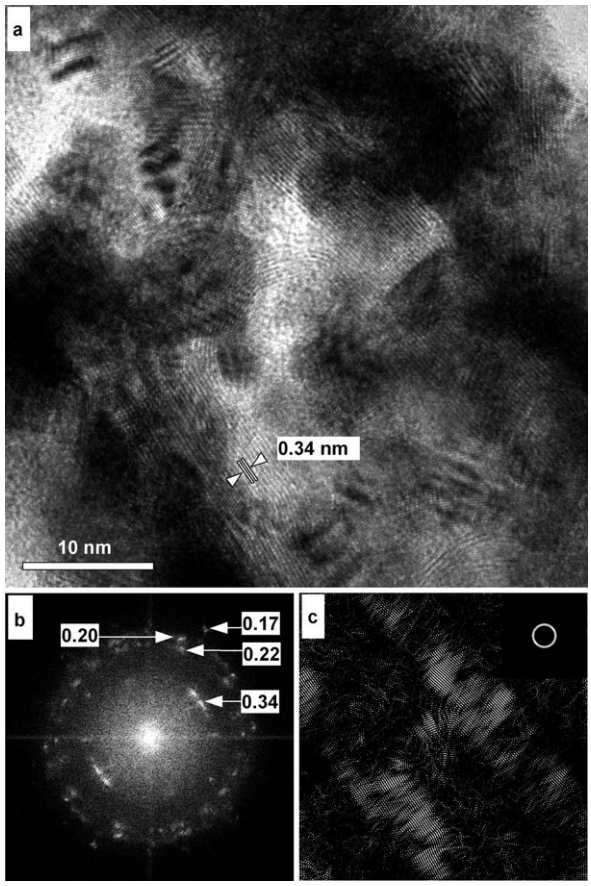

Figure 5. a) HRTEM image of a Ni-coated CNT. b) Fourier transform spot pattern of the image shown in (a). c) Reconstructed image obtained by inverse Fourier transformation after filtering out the spots from Ni and Pt with the mask shown in the inset (top right) to enhance the position of the CNT.

Since the CNT/Pt@Ni nanocomposites formed are exposed to an oxygen-containing environment during depo-

sition of the magnetic material, a stable NiO outer layer is expected to form which passivates the Ni shell and prevents full oxidation.[22] However, the presence of nickel oxides on the outer surface of the nickel nanotube could not be confirmed by the Fourier transform analysis shown in Figure 5. To determine whether nickel oxides were formed on the surface of the CNT/Pt@Ni nanocomposites the samples were examined by X-ray photoelectron spectroscopy (XPS; see the Supporting Information). Analysis of the Ni 2p peaks revealed a main peak for metallic Ni (852.8 eV) with contributions from different Ni oxidation states, presumably corresponding to the binding energies of NiO and $Ni(OH)_2$ (854.4 and 856.5 eV, respectively). These main lines are accompanied by satellite lines with binding energies that are 6 eV higher, which suggests the presence of these Ni oxides at the outer surface of the nickel wires. Apart from passivation, this surface oxidation process leads to ferromagnetic/antiferromagnetic (FM/AFM) interfaces (Ni/NiO), which give rise to an exchange bias effect that increases the potential applications of these nanocomposites.

The DC magnetic properties of these CNT/Pt@Ni/NiO nanocomposites were recorded in a SQUID magnetometer. Figure 6a shows the hysteresis curves collected at 5 K (field cooled (FC), 2 kOe) and at 300 K. The hysteresis loop at 5 K is shifted along the applied field direction, with an exchange bias field, H_E, of 72 Oe and a coercivity, H_C, of 380 Oe. The hysteresis loop at 300 K is open, with a coercivity of 91 Oe (Figure 6a). The exchange bias effect occurs owing to the exchange coupling at FM/AFM interfaces, which leads to a shift of the hysteresis loop along the applied field axis.

Exchange anisotropy, which was discovered by Meiklejohn and Bean,[23] refers to the properties of exchange-coupled FM/AFM materials and the effect is most simply manifested by an offset of the FC hysteresis loop from zero on the field axis. This exchange bias effect can therefore be expected to be the result of an exchange interaction between the uncompensated surface spins of NiO and metallic Ni in the Ni/NiO-coated CNT/Pt nanocomposites. This shift of the hysteresis loop can be established either by cooling the FM/AFM material in a magnetic saturation field below the Néel temperature of the antiferromagnet (2 kOe in this case) or by depositing both materials under an external magnetic field.[13] Figure 6b shows the 1-kOe field-cooled (FC) and zero-field-cooled (ZFC) magnetization curves as a function of temperature. The maximum in the ZFC curve at 40 K is usually ascribed to the average blocking temperature of the magnetic moment.

The ZFC and FC curves diverge at a maximum blocking temperature of 186 K, which corresponds to the largest nanotubes present in the sample. More detailed investigations of this magnetic behavior will be reported elsewhere. The magnetic nature of the nanocomposites was also shown by drying a drop of the dispersion on a Si wafer at 300 K under an applied magnetic field of 0.2 T, which resulted (Figure 6c) in their alignment into long chain structures through a magnetophoretic deposition process.

In summary, Ni hollow nanotubes have been grown using CNTs wrapped with charged polyelectrolytes and coated with Pt nanoparticles as templates while preserving the CNT

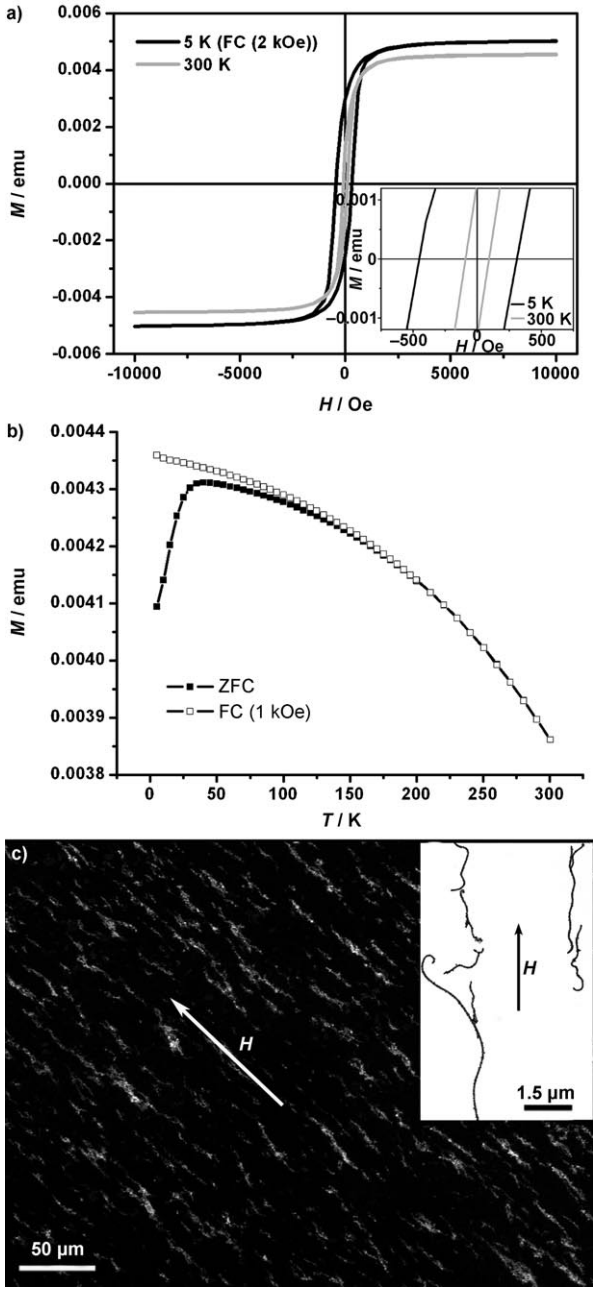

Figure 6. a) Hysteresis loops measured at 5 K (field-cooled, 2 kOe) and 300 K. b) Temperature dependence of the ZFC (close symbols) and FC (open symbols) magnetization measured at 1 kOe for the Ni/NiO-coated CNT/Pt nanocomposites. c) SEM image of the nanocomposites deposited on a Si substrate and aligned under an external magnetic field (arrow indicates direction) of 0.1 T. Inset: Higher magnification TEM image.

structure. The catalytic activity of the CNT-supported Pt nanoparticles has been used to control the reduction of metallic Ni onto their surface, along with a passivating NiO surface layer. The resulting anisotropic and magnetic Ni/NiO nanotube colloids are excellent candidates for use as building blocks for the fabrication of novel composite materials with a magnetic-field-driven preferential orientation. An additional advantage of this system stems from the fact that the magnetic CNT structures are stable in the absence of additional

stabilizers or surfactants and their magnetic properties permit their alignment under relatively low magnetic fields, which emphasizes their potential for further manipulation and assembly, for example in nanoreinforced fiber materials.

Experimental Section

CNT polyelectrolyte functionalization: CNTs were dispersed in ultra pure water (18 MΩ cm) following a published procedure.[3,4] Briefly, CNTs were dispersed in a 1 wt. % aqueous solution of polyallylamine hydrochloride (PAH) to a concentration of 150 mg L^{-1}. A combination of rapid stirring and sonication was used to ensure the presence of well dispersed, individual nanotubes. Excess PAH was removed by several centrifugation and redispersion cycles.

Platinum seeds: The Pt nanoparticles to be deposited onto CNTs were synthesized as follows. Sodium borohydride (2.9 mL, 0.06 M) was added as a reducing agent to a solution of sodium citrate (2.5 mL, 0.1 M) and K_2PtCl_4 (0.5 mL, 0.05 M) in ultrapure water (44 mL) and the resulting solution stirred for 10 min.

Pt deposition on the CNT surface: CNT@PAH (0.6 mL, 0.5 mg mL^{-1}) was added to a solution of Pt seeds (50 mL, 0.5 mM). After allowing to stand for 30 min, the solution was centrifuged (10 min, 8000 rpm) and redispersed in pure water (20 mL) to remove nondeposited nanoparticles.

Ni growth: The CNT/Pt dispersion (20 mL) was added to an aqueous solution (30 mL) containing an $NiCl_2$ stock solution (0.06 mL, 0.25 M) and hydrazine (0.12 mL, 2.5 M). The mixture was maintained at 40 °C for 2 h, then decanted with the help of a handheld magnet and washed with water and ethanol (twice for each solvent).

Received: April 16, 2007
Published online: August 14, 2007

Keywords: magnetic properties · materials science · nanotubes · nickel · platinum

[1] a) W. G. Wilder, L. C. Venema, A. G. Rinzier, R. E. Smalley, C. Dekker, *Nature* **1998**, *391*, 59; b) T. W. Odom, J.-L. Huang, P. Kim, C. M. Lieber, *Nature* **1998**, *391*, 62; c) M. M. J. Treacy, T. W. Ebbesen, J. M. Gibson, *Nature* **1996**, *381*, 678; d) M. J. O'Connell, S. M. Bachilo, C. B. Huffman, V. C. Moore, M. S. Strano, E. H. Haroz, K. L. Rialon, P. J. Boul, W. H. Noon, C. Kittrell, J. Ma, R. H. Hauge, R. B. Weisman, R. E. Smalley, *Science* **2002**, *297*, 593; e) M. Fujiwara, E. Oki, M. Hamada, Y. Tanimoto, I. Mukouda, Y. Shimomura, *J. Phys. Chem. A* **2001**, *105*, 4383.

[2] a) R. H. Baughman, A. A. Zakhidov, W. A. de Heer, *Science* **2002**, *297*, 787; b) P. Avouris, *Acc. Chem. Res.* **2002**, *35*, 1026; c) "Carbon Nanotubes Synthesis, Structure, Properties, and Applications": M. S. Dresselhaus, G. Dresselhaus, P. Avouris, *Top. Appl. Phys.* **2001**, 80; d) M. A. Correa-Duarte, N. Wagner, J. A. Rojas-Chapana, C. Morsczeck, M. Thie, M. Giersig, *Nano Lett.* **2004**, *4*, 2233; e) J. A. Rojas-Chapana, M. A. Correa-Duarte, Z. Ren, K. Kempa, M. Giersig, *Nano Lett.* **2004**, *4*, 985.

[3] M. A. Correa-Duarte, M. Grzelczak, V. Salgueirino-Maceira, M. Giersig, L. M. Liz-Marzán, M. Farle, K. Sierazdki, R. Diaz, *J. Phys. Chem. B* **2005**, *109*, 19060.

[4] a) M. Grzelczak, M. A. Correa-Duarte, V. Salgueiriño-Maceira, M. Giersig, R. Diaz, L. M. Liz-Marzán, *Adv. Mater.* **2006**, *18*, 415; b) M. A. Correa-Duarte, L. M. Liz-Marzán, *J. Mater. Chem.* **2006**, *16*, 22; c) M. A. Correa-Duarte, J. Pérez-Juste, A. Sanchez-Iglesias, M. Giersig, L. M. Liz-Marzán, *Angew. Chem.* **2005**, *117*, 4449; *Angew. Chem. Int. Ed.* **2005**, *44*, 4375; d) S. Banerjee, S. S. Wong, *Nano Lett.* **2002**, *2*, 195; e) S. S. Wong, E. Joselevich, A. T. Woolley, C. L. Cheung, C. M. Lieber, *Nature* **1998**, *394*, 52.

[5] a) V. F. Puntes, K. M. Krishnan, A. P. Alivisatos, *Science* **2001**, *291*, 2115; b) F. Dumestre, B. Chaudret, C. Amiens, M.-C. Fromen, M.-J. Casanove, P. Renaud, P. Zurcher, *Angew. Chem.* **2002**, *114*, 4462; *Angew. Chem. Int. Ed.* **2002**, *41*, 4286; c) F. Dumestre, B. Chaudret, C. Amiens, M. Respaud, P. Fejes, P. Renaud, P. Zurcher, *Angew. Chem.* **2003**, *115*, 5371; *Angew. Chem. Int. Ed.* **2003**, *42*, 5213; d) C. Goubault, F. Leal-Calderon, J.-L. Viovy, J. Bibette, *Langmuir* **2005**, *21*, 3725.

[6] a) V. Salgueiriño-Maceira, M. A. Correa-Duarte, A. Hucht, M. Farle, *J. Magn. Magn. Mater.* **2006**, *303*, 163; b) S. Sacanna, A. P. Philipse, *Langmuir* **2006**, *22*, 10209; c) F. Martínez Pedrero, M. Tirado Miranda, A. Schmitt, J. Callejas Fernández, *J. Chem. Phys.* **2006**, *125*, 084706; d) B. D. Korth, P. Keng, I. Shim, S. E. Bowles, C. Tang, T. Kowalewski, K. W. Nebesny, J. Pyun, *J. Am. Chem. Soc.* **2006**, *128*, 6562; e) M. Klokkenburg, R. P. A. Dullens, W. K. Kegel, B. H. Erné, A. Philipse, *Phys. Rev. Lett.* **2006**, *96*, 037203; f) G. Cheng, D. Romero, G. T. Fraser, A. R. Hight Walker, *Langmuir* **2005**, *21*, 12055; g) E. M. Claesson, A. P. Philipse, *Langmuir* **2005**, *21*, 9412.

[7] K. Ahrenstorf, O. Albrecht, H. Heller, A. Kornowski, D. Görlitz, H. Weller, *Small* **2007**, *3*, 271.

[8] J. Jacob, W. A. Goddard, *J. Phys. Chem. B* **2004**, *108*, 8311.

[9] a) K.-W. Park, J.-H. Choi, B.-K. Kwon, S.-A. Lee, Y. E. Sung, H.-Y. Ha, S.-A. Hong, H. Kim, A. Wieckowski, *J. Phys. Chem. B* **2002**, *106*, 1869; b) K.-W. Park, J.-H. Choi, Y.-E. Sun, *J. Phys. Chem. B* **2003**, *107*, 5851.

[10] M. Yang, Y. Yang, F. Qu, Y. Lu, G. Shen, R. Yu, *Anal. Chim. Acta* **2006**, *571*, 211.

[11] A. K. Bentley, A. B. Ellis, G. C. Lisensky, W. C. Crone, *Nanotechnology* **2005**, *16*, 2193.

[12] D. H. Reich, M. Tanase, A. Hultgren, L. A. Bauer, C. S. Chen, G. J. Meyer, *J. Appl. Phys.* **2003**, *93*, 7275.

[13] M. Fraune, U. Rüdiger, G. Güntherodt, S. Cardoso, P. Freitas, *Appl. Phys. Lett.* **2000**, *77*, 3815.

[14] M. J. O'Connell, P. Boul, L. M. Ericson, C. Huffman, Y. Wang, E. Haroz, C. Kuper, J. Tour, K. D. Ausman, R. E. Smalley, *Chem. Phys. Lett.* **2001**, *342*, 265.

[15] N. A. Kotov, T. Haraszti, L. Turi, G. Zavala, R. E. Geer, I. Dekany, J. H. Fendler, *J. Am. Chem. Soc.* **1997**, *119*, 6821.

[16] F. Bottomley, *Q. Rev. Chem. Soc.* **1970**, *24*, 617.

[17] S.-H. Wu, D.-H. Chen, *Chem. Lett.* **2004**, *33*, 406.

[18] A. V. Anan'ev, M. Y. Boltoeva, N. L. Sukhov, G. L. Bykov, B. G. Ershov, *Radiochemistry* **2004**, *46*, 578.

[19] J. L. Gland, G. B. Fisher, G. E. Mitchell, *Chem. Phys. Lett.* **1985**, *119*, 89.

[20] C. Kiang, M. Endo, P. Ajayan, G. Dresselhaus, M. Dresselhaus, *Phys. Rev. Lett.* **1998**, *81*, 1869.

[21] A. Charlier, E. McRae, R. Heyd, M. Charlier, D. Moretti, *Carbon* **1999**, *37*, 1779.

[22] A. Roy, V. Srinivas, S. Ram, J. A. de Toro, U. Mizutani, *Phys. Rev. B* **2005**, *71*, 184443.

[23] a) W. H. Meiklejohn, C. P. Bean, *Phys. Rev.* **1956**, *102*, 1413; b) W. H. Meiklejohn, *J. Appl. Phys.* **1962**, *33*, 1328.

